

## Numerical analysis on Buried pipes protected by combination of geocell reinforcement and rubber-soil mixture

Gh. Tavakoli Mehrjardi<sup>1,\*</sup>, S.N. Moghaddas Tafreshi<sup>2</sup>, A.R. Dawson<sup>3</sup>

Received: July 2014, Accepted: May 2015

### Abstract

A numerical simulation of laboratory model tests was carried out to develop an understanding of the behaviour of pipes in a trench prepared with 3-Dimensional reinforced (namely "geocell-reinforced" in the present study) sand and rubber-soil mixtures, under repeated loadings. The study reports overall performance of buried pipes in different conditions of pipe-trench installations and the influence of pipe stiffness on backfill settlements, stress distribution in the trench depth and stress distribution along the pipe's longitudinal axis. Good agreements between the numerical results and experimental results were observed. The results demonstrate that combined use of the geocell layer and rubber-soil mixture can reduce soil surface settlement and pipe deflection and eventually provide a secure condition for buried pipe even under strong repeated loads.

**Keywords:** Numerical analysis, Geocell, Buried pipes, Rubber-soil mixture, Stress transfer.

### 1. Introduction

Buried pipeline systems are classified as 'lifelines' since they carry essential materials for the support of human life [1]. Therefore, damage of these systems can result in heavy loss of functionality with the consequential interference to the economic and social recovery in the areas where the damage occurred and, also, at the end of the 'lifeline', possibly allowing illnesses and epidemics to develop. In order to prevent damage of such pipes, they must be placed deep enough, and under well-compacted trench backfill [2, 3].

With the increased use of vehicles comes an increase in the numbers of waste tires. Safe, beneficial use of this rubber underground not only overcomes disposal problems but is also beneficial for the rubber, from an environmental point of view, as it is removed from sunlight which may cause its degradation. Also, many advantages of using soil and rubber mixtures in geotechnical applications have been reported [4-9]. The material may be used around buried pipes and, potentially, can ensure the protection of both the pipe and itself for the long-term, keeping the rubber in an environmentally beneficial end-application [10].

The beneficial ability of cellular geosynthetic mattress constructions to improve the bearing capacity and settlement of footings has been reported by several authors [11-16]. Appropriate geocell reinforcement of soil, trench backfill or granular pavement construction over pipes seems likely to have the possibility of reducing the stress imposed on the pipe [17-18].

Some researchers studied the behavior of fiber-reinforced soil and geocell-reinforced soil separately by computational methods. Babu et al. (2008) [19] proposed an approach for considering the effect of random-oriented fibres in numerical analyses. The mechanisms by which random fibre-reinforced sand are explained in terms of a microstructure that prevents the formation of distinct localized strain bands and increases pull-out resistance. Saride et al. (2008) [20] carried out a numerical simulation of laboratory model tests to develop an understanding of the behaviour of geocell-reinforced sand, and soft clay foundation beds under a circular footing. The influence of the geometrical parameters of the geocell (width,  $b$ , and height,  $h$ ) on the overall performance of the footing was investigated. The results demonstrated that the geocell mattresses redistributed the footing pressure over a wider area thereby improving the performance of the footing. The pressure-settlement responses corresponding to geocell-reinforced beds were found to be much stiffer in comparison with an unreinforced case indicating that a substantial reduction in footing settlement can be ascertained. Also, Leshchinsky and Ling (2013) [21] investigated the effects of geocell confinement on ballasted embankments by numerical modelling. The composite effect of the confined ballast, selected as infill, may be economical by allowing the use of weaker/inferior

\* Corresponding author: ghtavakoli@khu.ac.ir

<sup>1</sup> Assistant Professor, Department of Civil Engineering, Kharazmi University, Tehran, Iran

<sup>2</sup> Professor, Department of Civil Engineering, K.N. Toosi University of Technology, Tehran, Iran

<sup>3</sup> Associate Professor, Nottingham Transportation Engineering Centre, University of Nottingham, Nottingham, UK

ballast, by requiring less embankment maintenance over problem soils, by improving the bearing capacity and by reducing the foundation settlement.

This paper seeks to investigate more efficient, yet still reliable backfill for such lifeline pipe installations by drawing on two relatively new concepts in combination – post-consumer rubber and cellular geosynthetic mattress reinforcement. This is achieved by the use of numerical simulations, using the FLAC-3D computational code, that reproduce full-scale model tests of a pipe-trench system prepared with geocell-reinforced sand and rubber-soil mixtures that were subjected to repeated loading simulative of over-running heavy traffic. As a whole, this study in compared with the full-scale model tests, exhibited further study to understand the behaviour of buried pipe system in different backfill materials and at different loading conditions, the stress distribution in the backfill mass, deformed shape of the pipe under transferred stress and etc. which not easily achievable using experimental model.

## 2. Experimental Studies

A series of full-scale tests were carried out to investigate the decrease of strain in buried flexible service pipes and of the settlement of backfill over such pipes by the use of geocell reinforcement (a 3D-inclusion reinforcement) with rubber-soil mixtures under repeated

loading conditions. Herein, only the essential features are discussed and more details on the test set-up, testing procedure, loading conditions and materials can be found in the authors' previous papers [10, 17-18].

A full-scale test site at University of Nottingham known as the Nottingham Pavement Test Facility (PTF) was used to provide realistic test conditions [22]. The schematic representation of the model test setup and its attachments comprising a test trench, loading system, and data measurement system (soil pressure cells at points of A, B, C and strain gauges at points A, B) is shown in Fig. 1. The full scale model test was constructed with plan dimensions of 6000 mm × 1100 mm (6000 mm in width in X direction and 1100 mm in length in Y direction, the longitudinal axis of the pipe) and a re-instatement trench (backfill soil) with section dimensions of 500 mm × 480 mm (500 mm in width in X direction and 480 mm in height in Z direction, Fig. 1). The base of the PTF is at about 1600 mm depth, but only 480 mm of this was excavated to install the pipe and backfill (see Fig. 1). The trench width of 500 mm was selected in the line with the recommendations of ASTM D2321 (2008) [21] and BSI (1980) [24]. Furthermore, the buried depth of the pipe was selected as two times the pipe's diameter (=320 mm) as proposed by Moghaddas Tafreshi and Tavakoli (2008) [25] being an optimized value of burial depth for a pipe embedded in geogrid-reinforced soil.

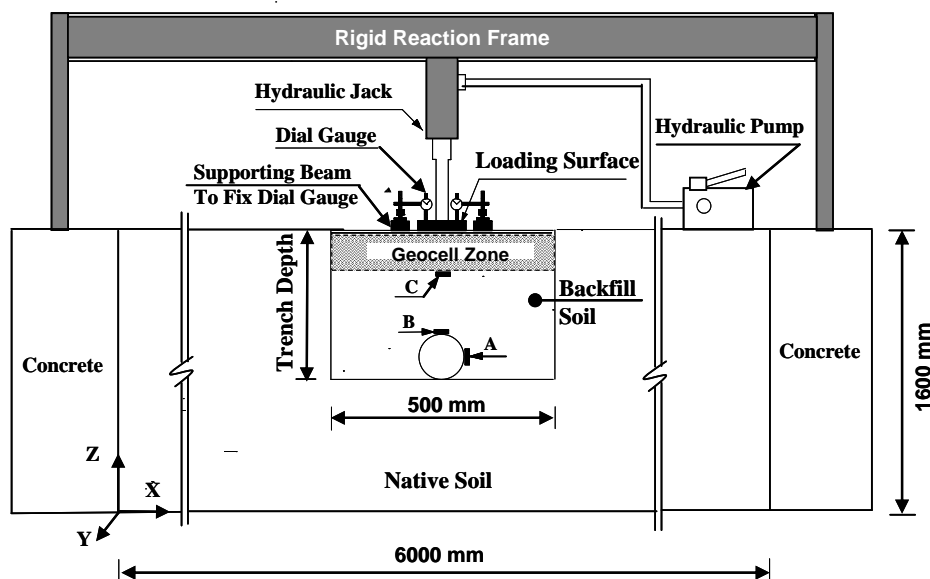


**Fig. 1** Schematic representation of the test setup (Not to scale).  
 “A, B = location of soil pressure cells and strain gauges; C = location of soil pressure cell”

Two types of granular soil, namely “native” soil and “backfill” soil (without rubber) are used to simulate the native ground adjacent to the trench and the buried pipe coverage respectively. The properties of these soils, which are classified as SW in the Unified Soil Classification System, are given in Table 1.

**Table 1** Physical properties of native and backfill soil

Description	Backfill soil	Native soil
Coefficient of uniformity, $C_u$	11.11	31.11
Coefficient of curvature, $C_c$	1.44	1.78
Medium grain size, $D_{50}$ (mm)	4	8
Specific gravity, $G_s$	2.65	2.67

The tests were conducted on uPVC pipe that complies with BSI 4660. The pipe has an outer diameter (D) of 160 mm, wall thickness (t) of 4 mm (a Standard Dimension Ratio =  $D/t = 40$ ) and 1100 mm length. The tensile strength at 10% axial strain and the Poisson's ratio of the pipe were 22 MPa and 0.46, respectively. The geocell had

the pocket size and height of  $100 \times 100 \text{ mm}^2$  and 100 mm, respectively and a tensile strength of 21.3 kN/m.

All the tests are divided into two group of installations namely "first installation" and "second installation" to calibrate and then validate the numerical model, respectively (Fig. 2 and Table 2).

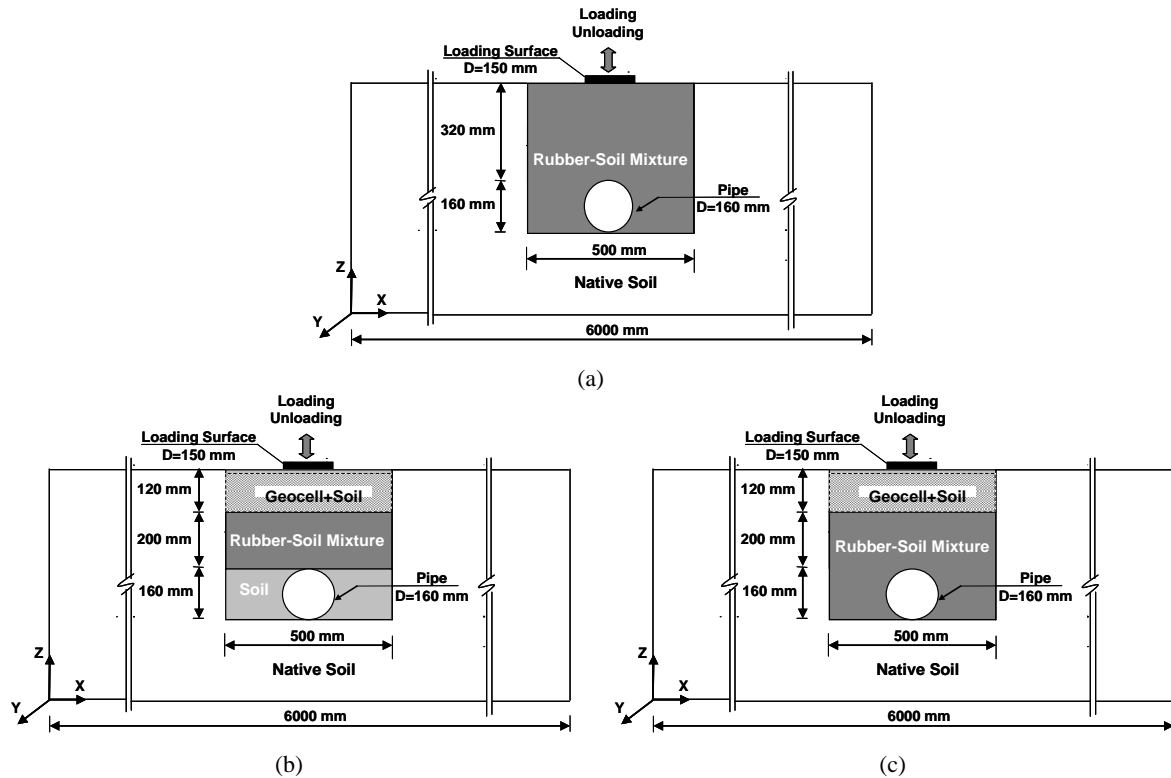


**Fig. 2** Schematic view of combined geocell reinforcement and rubber-soil mixture tests; (a) first test installation applicable for numerical model calibration; (b) mixture over the pipe ("Over") in second test installation; and (c) mixture around and over the pipe ("Whole") second test installation. (Not to scale)

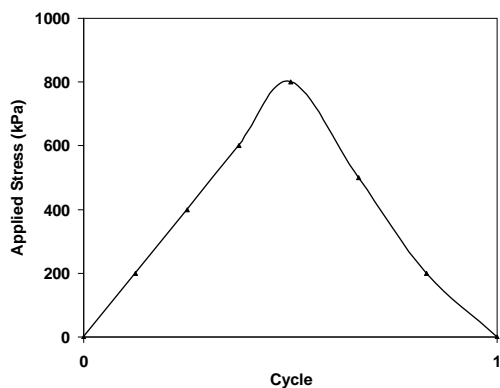
**Table 2** Testing programme

Test Installation	Test Configuration	Rubber Content (%)	Mixture Location	Reinforcement Status
First Installations	No Rubber	0	None	Unreinforced
		0	None	Reinforced
	Chipped Rubber	5, 10, 20	All Trench	Unreinforced
	Shredded Rubber	5, 10, 20	All Trench	Unreinforced
Second Installations		5	Over; Whole	Reinforced; Unreinforced
	Chipped Rubber	10	Over; Whole	Reinforced; Unreinforced
		20	Over	Unreinforced
		5	Over	Reinforced; Unreinforced
	Shredded Rubber	10	Over; Whole	Reinforced; Unreinforced
	20	Over	Unreinforced	

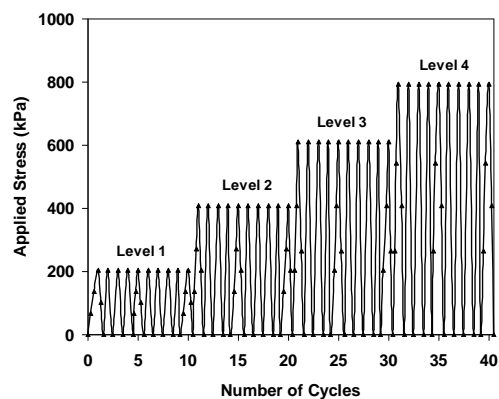
The schematic representation of both installations and their inclusions is shown in Fig. 2. In the first installation, the location of the backfill was from the bottom to the surface of the trench (Fig 2a) and also only one loading and unloading were applied on the trench surface (Fig. 3a).

In this installation, the backfill can be soil only or soil with 5, 10 and 20 percent (by mass) of shredded (S) or chipped (C) rubber-soil mixture. In the second installation (Figs. 2b and 2c) two rubber sizes (namely chipped ("C") and shredded ("S") rubbers), three different percentages of

rubber content in the mixture by mass (5%, 10% and 20%), two locations for soil-rubber mixture inside the trench (namely "over" (abbreviated to "O") indicating a thickness of 200 mm over the pipe and "whole" (abbreviated to "W") indicating that the mix is used both around and over the pipe at the same thickness), four levels of repeated loading (200, 400, 600 and 800 kPa) and the addition ("Re") or not ("Ur") of geocell reinforcement over the pipe are the variables considered (Fig. 3b). For



(a)



(b)

**Fig. 3** Loading patterns for (a) first installation; (b) second installation

### 3. Numerical Analysis

The numerical simulations for the analysis of pipe buried in trench were performed using the finite difference code FLAC-3D (2002) [26]. Since the experimental study presented is only for one kind of pipe, the influence of pipe stiffness on backfill settlements and on the stress distributions through the trench depth and along the pipe's longitudinal axis were investigated by numerical simulations. The geometry of the model, its calibration, its verification and a parametric study are discussed in the following sections.

#### 3.1. Model geometry

The dimensions of the simulated model replicated those of the experimental model (see Fig. 1). As the model is symmetrical about the X-Z plane, only a half geometry was assumed in all simulations, with the plane of symmetry replaced by a vertical boundary constrained to have no horizontal displacement. The domain was divided into 17200 mesh 'openings' connected by 19866 grid points, organized in radial and brick patterns. The media around the pipe was divided into the primitive mesh shape named a "radcylinder" which is a radially graded mesh around the pipe to maintain the compatibility between the pipe and the soil, as shown in Fig. 4a. The pipe was divided into the primitive shell-element mesh and the trench walls and bed were modelled with cubic, "brick", elements. Owing to use of plain wall pipe, to the nature of loading and to the type of backfill used, no interface was considered between backfill and pipe.

The boundary conditions, applied in the numerical models are shown in Fig. 4b. The displacement of the

example, the installation "C(5%)O-Ur" means that the backfill was the mixture of soil with 5% chipped rubber by weight which was located over the pipe (see Fig. 2b) and also the trench was filled in without geocell reinforcement. The details of the testing program for first and second installations are given in Table 2.

The loading and unloading patterns in both first and second installations as then used in the numerical modelling are shown in Fig. 3.

outer boundary was restrained in X and Y directions and that of the base was restricted in all directions.

#### 3.2. Material properties

The pipe's material was assumed to be linear-elastic and its parameters such as elasticity modulus and Poisson's ratio, were obtained by a tensile strength test on a belt sample of the pipe. As the trench walls and bed were constructed with cohesive-frictional well-graded sands and heavily compacted, and because the walls are far from the footing, the pipe behaviour was considered elastic. The bulk and shear modulus of trench's sides, measured by light weight deflectometer testing (LWD), were evaluated as 350 and 290 MPa.

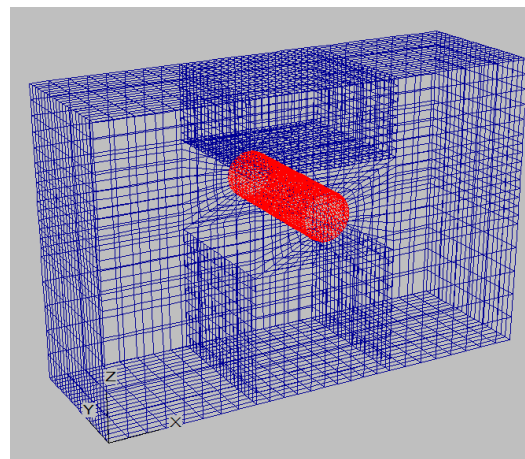
The backfill soil was cohesive-frictional well-graded sands which its cohesion and friction angle, obtained by triaxial tests, were 22 kPa and 38 degree, respectively. Some additional full-scale tests (second installations) were performed to assess the backfills (unreinforced soil (Ur), rubber-soil mixture and geocell-reinforced soil (Re)) as composite materials. An elastic-perfectly plastic associative Mohr-Coulomb constitutive model was used to simulate the behaviour of each. Even though more sophisticated elasto-plastic constitutive models exist, Mohr-Coulomb model is deemed satisfactory in the present case as the anticipated stress paths are mainly dominated by shear failure when significant load is applied on the soil sample. To calibrate the parameters of the chosen plasticity model, the following points were considered:

a) Geocell-reinforcement of a soil results, in part, in the generation of apparent cohesion. An experimental study performed by Rajagopal et al. (1999) [27] showed the development of an apparent cohesion even when using geocell in a non-cohesive soil. In addition the friction is increased to some extent [28].

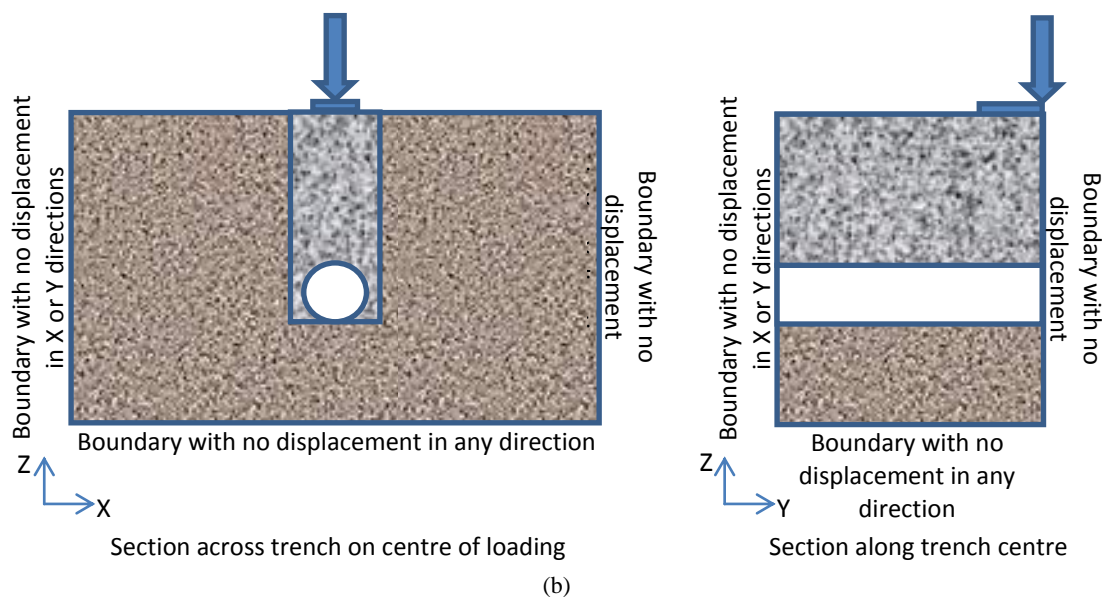
b) Gotteland et al. (2005) [29] investigated some triaxial tests on rubber-soil mixture and found that, with an

increasing proportion of rubber volume in samples, the trend of most specimens was to yield a decrease of both cohesion and friction angle.

c) The dilation angle of all composites was assumed to be two-third of the value of friction angle in the corresponding composite material as suggested by Erickson and Drescher (2002) [30].



(a)



(b)

**Fig. 4** Simulated model with (a) Geometry of model; (b) Boundary conditions

### 3.3. Model calibration

To calibrate the parameters, the numerical model was used to replicate the full-scale tests in first installations. This was done progressively with, firstly, the trench's walls and floor being simulated and analyzed under gravitational body forces (Fig. 5a). Then, the pipe was

located in its place, the backfill over the pipe, displacements set to zero and the program used with gravitational body forces. Fig 5b shows the pipe deflection in z-direction at the end of this step for soil only backfill. Finally one cycle of loading and unloading (see Fig. 3a) was applied on the trench surface to complete the simulation process (Fig 5c and 5d).

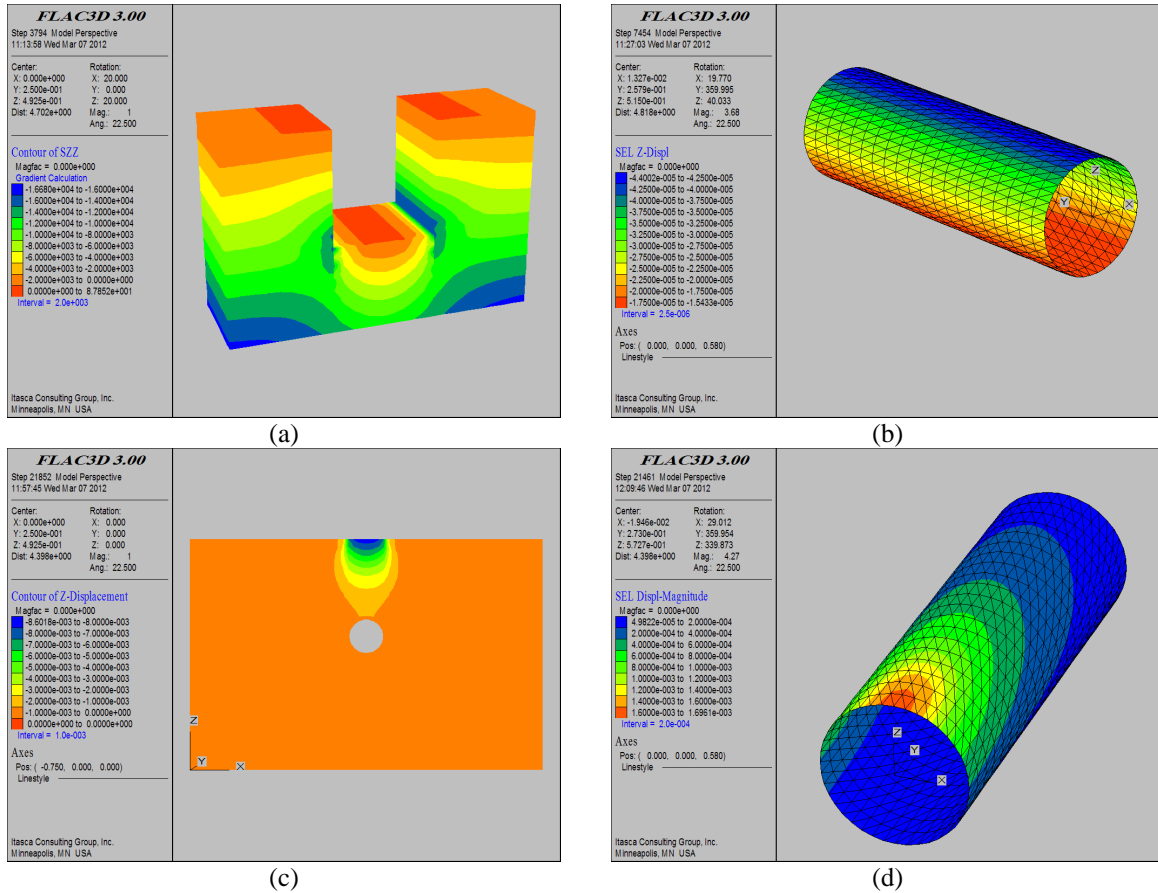


**Fig. 5** Model Calibration (a) Stress in trench's wall under gravitational body forces, (b) Pipe's deflection under backfill loads, (c) Settlements in trench under one cycle of loading, and (d) Pipe's deflection under one cycle of loading

By using a trial-and-error technique, adjusting the input parameters until the results of these numerical analysis closely matched those obtained from experimental model (Fig. 2a), representative values of bulk modulus ( $K$ ), shear

modulus ( $G$ ), cohesion ( $c$ ), friction angle ( $\phi$ ), dilation angle ( $\psi$ ) and density ( $\rho$ ), were obtained. The properties of the composites are presented in Table 3.

**Table 3** Details of material properties used in the present study obtained from calibration

Backfill	$K(MPa)$	$G(MPa)$	$c(kPa)$	$\phi(^{\circ})$	$\psi(^{\circ})$	$\rho(kN/m^3)$
Soil Only (Ur)	16	7	22	33	20	18.5
Soil Only (Re)	42	20	27	45	30	18
Chipped (5%)	6	2.8	15	30	18	12
Chipped (10%)	4.5	1.9	12	24	15	10
Chipped (20%)	1	0.4	7	15	10	8
Shredded (5%)	10	4.3	20	31	20	13
Shredded (10%)	7	3	14	30	18	11
Shredded (20%)	4.5	1.9	8	20	13	10

Fig. 6 compares the results obtained from these calibration numerical simulations with the experimental data measured from the same test configurations. To ensure satisfactory results provided by numerical model, all the parameters were calibrated to approach the nearest

values of soil surface settlement of the trench (SSS) and vertical diametral strain of the buried pipe (VDS) acquired from the experimental model. As can be seen, there is a generally a good match between the numerical results and the physical tests for all backfills.

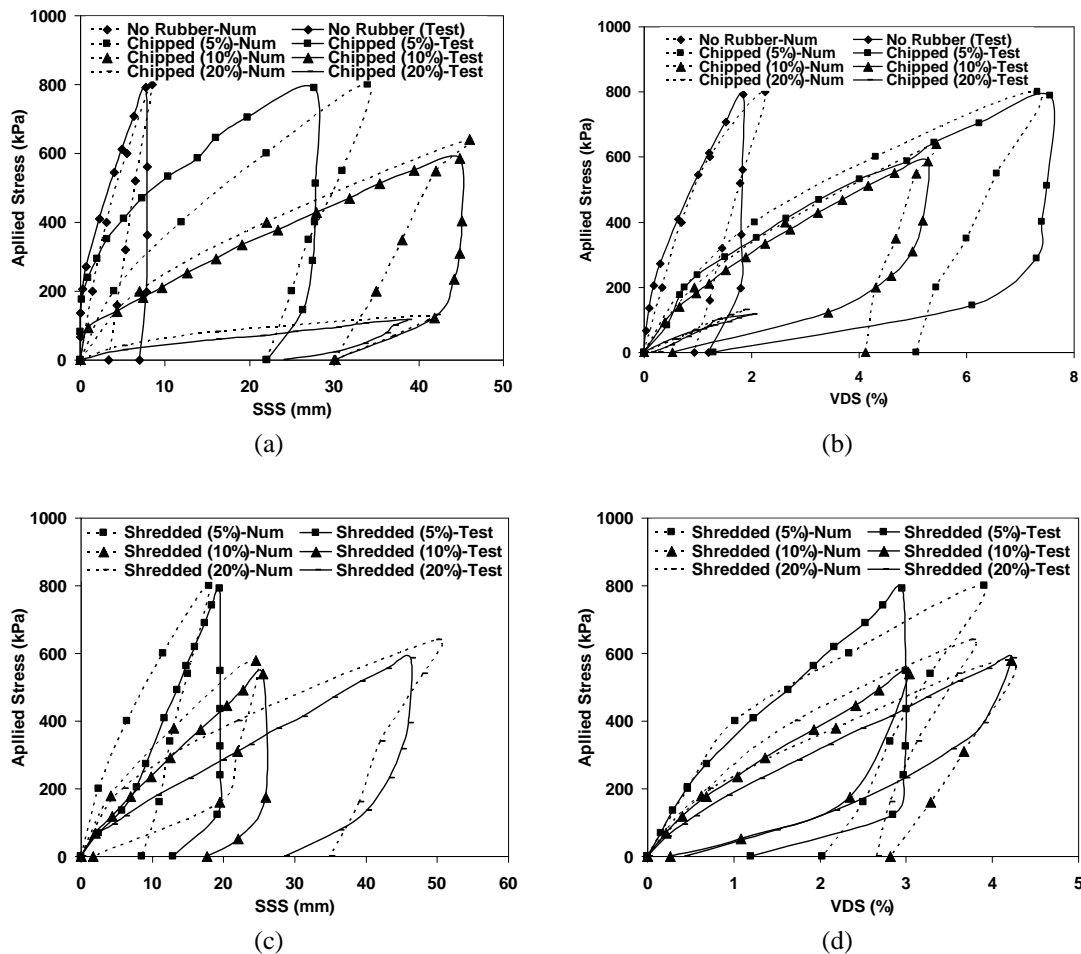


**Fig. 6** Comparison between numerical and experimental results at calibration stage (a) SSS values for chipped rubbers, (b) VDS values for chipped rubbers, (c) SSS values for shredded rubbers, (d) VDS values for shredded rubbers

### 3.4. Model verification

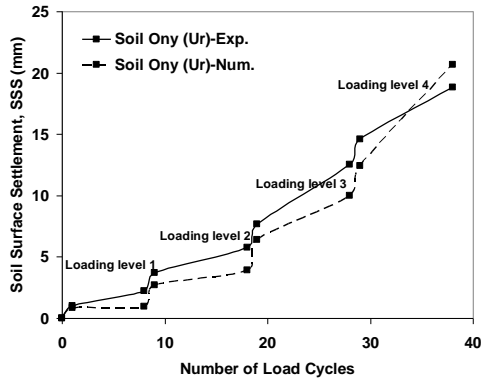
After calibration, the materials with the characteristics presented in Table 3 were used to model the second installation tests. To simulate the cyclic loading, the program was processed for each loading and unloading cycle, until the unbalance force reached a small value. It should be notified in the experimental tests, high frequency repeated loading and unloading was not employed [29]. Figs. 7 to 10 illustrate a small part of results in this stage of the study. Figs. 7 and 8 compare soil surface settlements and vertical diametral strain. A good match can be observed between numerical and experimental results. Figs. 9 and 10 are presented to show how the shear strain and vertical stress in the trench depth are distributed.

By comparing Figs. 7a, 7c and 7d, it is found that the mixture of chipped rubber and soil produces a more deformable material than soil only, tending to increase the soil surface settlement. Figs. 8c and 8d illustrate the influence of the chipped rubber-soil mixture's location on the response of the trench-pipe system. Due to providing a softer lateral support for buried pipes in the "whole" installation, vertical diametral strain was increased in this installation rather than in the "over" installation. This is in-

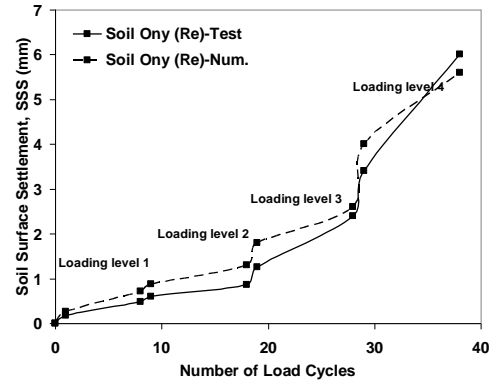
line with the findings of Rogers et al. (1995) [32] who reported that the pipe deflection in a narrower trench was decreased due to the provision of a stiffer lateral support for buried pipe.

The result presented in these figures show that, with installation of a geocell layer in the trench over the pipe, the soil surface settlement and vertical diametral strain of pipe could be attenuated by 68% and 33% respectively in comparison with those in an unreinforced trench.

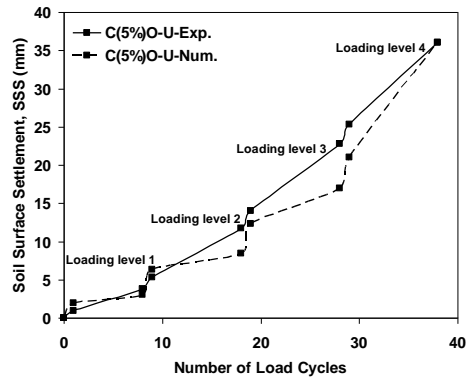
By comparing the shear strains in the soil-only ( $U_r$ ) and reinforced soil-only ( $Re$ ) installations in Figs 9a and 9b respectively, it is clear that the geocell layer can reduce the spread and intensity of shear strain under the footing, also tending to reduce both soil surface settlement and pipe deflection. On the other hand, by comparing Figs. 10a and 10b, it is seen that the geocell layer can successfully reduce the vertical stress on the pipe's crown from 90 kPa in unreinforced soil to 68 kPa in reinforced soil. Also, it is obvious that the stress 'shadow' over the pipe in C(5%)O- $U_r$  and C(5%)W- $U_r$  has spread deeper than the soil only. Therefore, the vertical stress transferred onto the pipe's crown has a larger value than that in the soil only ( $U_r$ ) and can be expected to make the pipe deflect more.



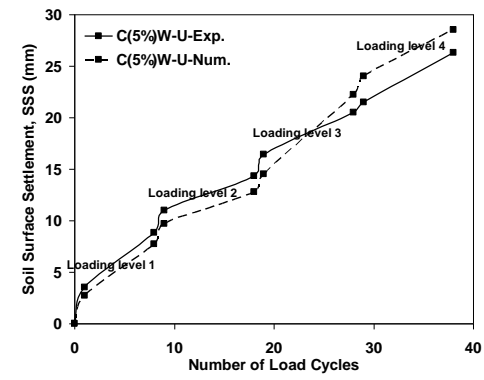
(a)



(b)

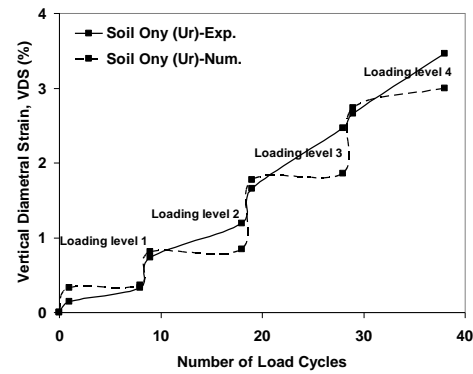


(c)

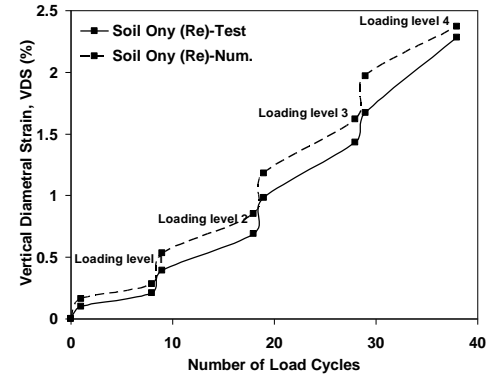


(d)

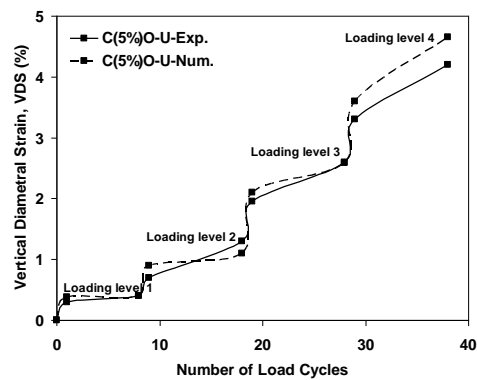
**Fig. 7** Comparison of soil surface settlements obtained from numerical and experimental results for a) Soil Only (Ur) b) Soil Only (Re) c) C (5%) O-Ur, and d) C (5%) W-Ur



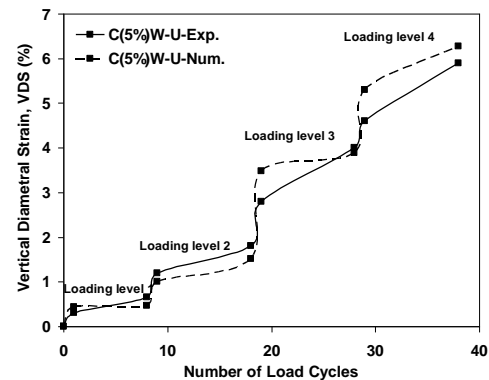
(a)



(b)



(c)



(d)

**Fig. 8.** Comparison of pipe's vertical diametral strain obtained from numerical and experimental results for a) Soil Only (Ur) b) Soil Only (Re) c) C (5%) O-Ur, and d) C (5%) W-Ur



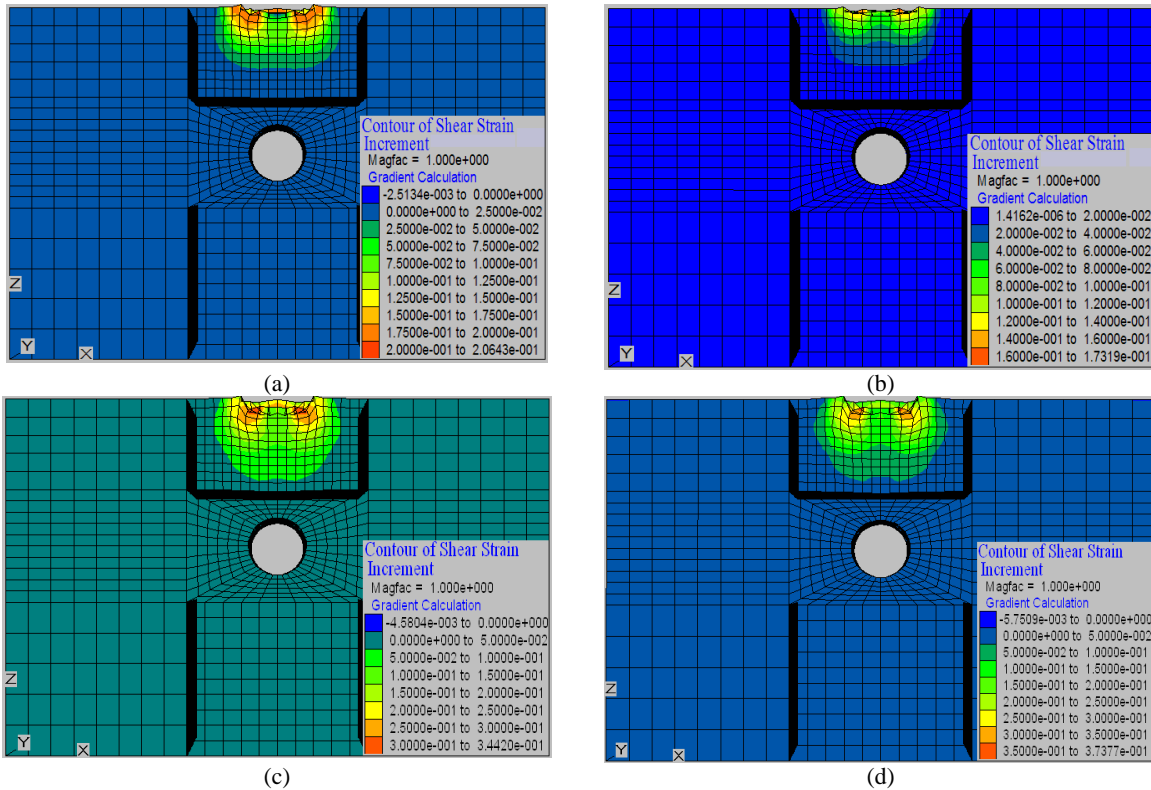


**Fig. 9** Shear strain contours obtained from numerical results for a) Soil Only (Ur) b) Soil Only (Re) c) C(5%) O-Ur, and d) C (5%) W-Ur

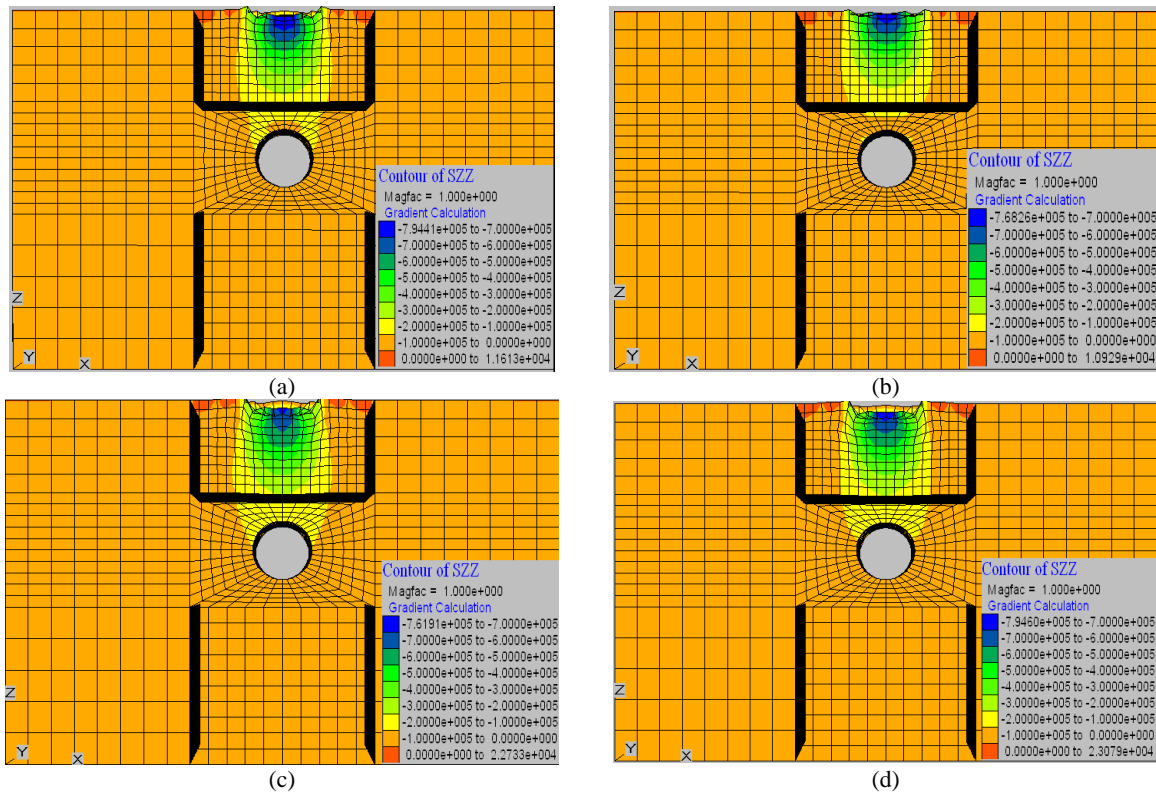


**Fig. 10** Vertical stress contours obtained from numerical results for a) Soil Only (Ur) b) Soil Only (Re) c) C(5%)O-Ur, and d) C(5%)W-Ur

#### 4. Results and Discussion

The above comparisons reveal that numerical analyses based on FLAC 3D can simulate reasonably well the performance of buried pipe in different backfill conditions

under repeated loadings. In this section, parametric studies are carried out to determine the response of buried pipes in rubber-soil mixtures and the influence of pipe stiffness on the soil settlements, stress distribution in the soil and along the pipe's longitudinal axis.

#### 4.1. Backfill and its position to the pipe

Werkmeister et al. (2004) [33] and Arnold (2004) [34] proposed a criterion to discern different forms of response of materials under cyclic loading on the basis of vertical permanent strain rate. Specifically, by plotting vertical permanent strain per load cycle, they divided the behaviour of base course materials into three different categories: Range A, Range B, or Range C. As can be seen from Fig. 11, Range A is the plastic shakedown range in which the granular material shows high strain rates per load cycle for a finite number of load applications during the primary stage but eventually plastic strain under repeated loading ceases and the material behaves in a purely resilient manner. The permanent strain in Range A is caused by the sample densification and particle rearrangement. Under higher stress cycles, range B appears. During this stage, the deformation of a granular material results from the relative interparticle movement and the deformation of the particle themselves [35]. Deformation never entirely ceases but continues, albeit at a very small rates. Finally, Range C is the incremental collapse shakedown range, caused by the grain abrasion and particle crushing, where relatively large-scale particle reorientation occurs, resulting in an unstable aggregate skeleton and large plastic strain rate [36].

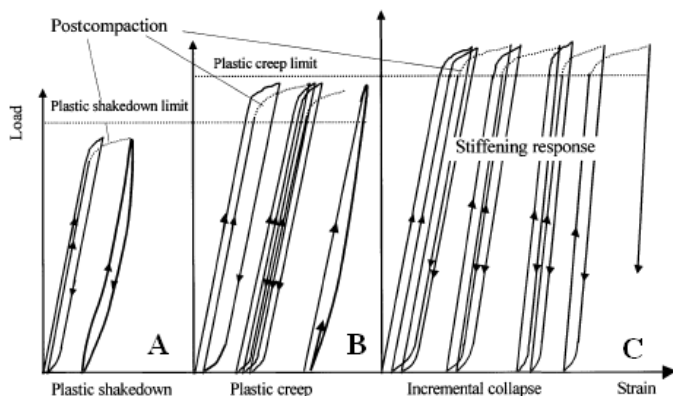


Fig. 11 Idealized behavior of granular materials under repeated cyclic pressure load [34]

To apply the shakedown theory in the present study, Fig. 12 shows the plastic deformation of the backfills (derived from soil surface settlements) in the unreinforced installations during the applied load cycles. The value printed at the end of each graph states the soil surface settlement at the end of the corresponding test. Clearly, the rate of plastic settlement of the backfill increased with number of load cycles. Also, for the tests having more than 25mm final soil surface settlement, the accumulated plastic deformations rose very rapidly after the second level of loadings (applied pressure > 400 kPa) such that shakedown Range A behaviour is not achieved, resilient behaviour does not appear and plastic deformation rapidly develops. There were insufficient numbers of loadings applied to determine whether the any of the large deformation responses would have eventually stabilized

(i.e. Range B behaviour) or whether they would have accelerated to collapse (Range C). However, it seems, surprisingly, that the "S(5%)O-Ur" installation has a Range A response, with the accumulated strain being rather small until a fully resilient behaviour is achieved. The "S(10%)O-Ur" installation has a Range B response with a continuing, but small, accumulation of plastic strain over many cycles of loadings. The soil-only installation has a response which appears to lie on the border of Ranges A and B. Werkmeister et al. (2004) [33] stated that Range C behaviour should not be allowed to occur in the pavement whereas Range B could be tolerated for a limited number of loading cycles or in roads that can be readily maintained (e.g. unsealed pavements).

Fig. 12 also explains that adding rubber particles, irrespective of size and with the exception of 5% shredded rubbers by weight, made the backfill more compressible than the soil alone (Fig. 12).

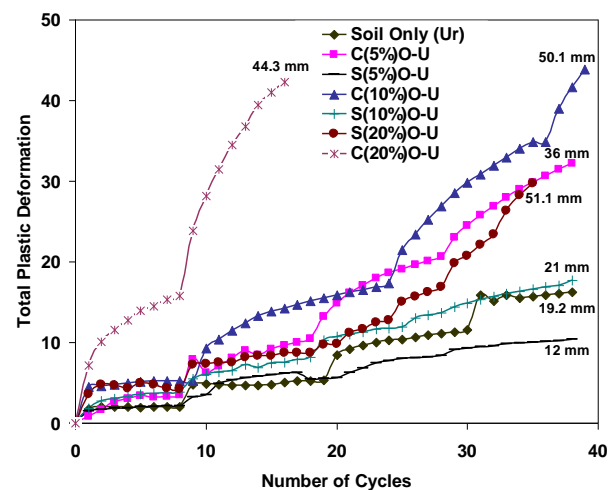


Fig. 12 Variations in accumulated plastic deformations of the backfills during applied load cycles

Flexible pipe products have a deflection design limit [38]. As can be seen from Fig. 13, the buried pipe under imposed load, firstly, deforms to an elliptical shape (Fig. 13a) and then, with increasing the external loads, the reversal of curvature or heart-shape develops (Fig. 13b) indicating the onset of pipe failure.

To investigate the pipe's deflection in different installations, the cross section of the tested pipes, with deformations at four-time magnification, at the last cycle of load application for unreinforced and geocell-reinforced of different backfills is shown in Fig. 14. As can be seen, pipe in the "C(20%)O-Ur" unreinforced installation (Fig. 14a) tends to gain a heart-shape deformation that is associated with a high bending moment at the crown of the pipe. Also, due to lack of enough lateral support for pipe buried in the "C(10%)W-Ur" installation, the shape of pipe was over-deflected. However, the results captured in Fig. 14c show the ability of the geocell to attenuate the pipe deflection both at crown and springline of the pipe and conceivably, prevent the pipe suffering a reversal of its curvature.

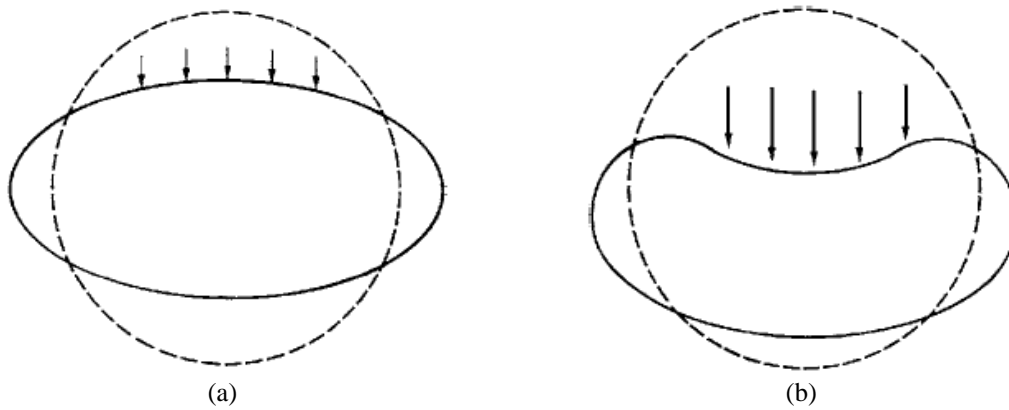


Fig. 13 Ring deflection in a flexible pipe (a) elliptical shape cross section, (b) reversal of curvature (heart-shape cross section) [35]

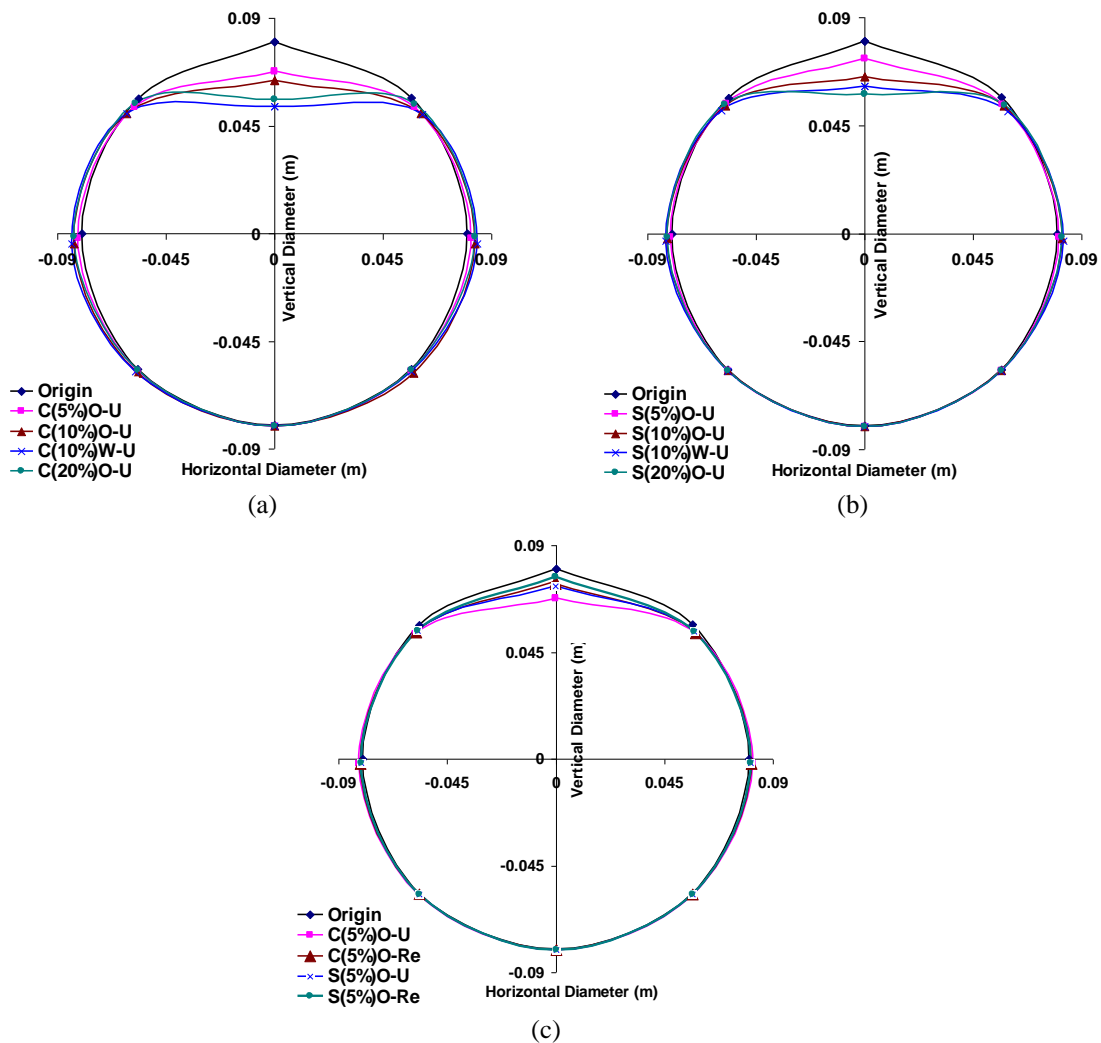


Fig. 14 Deformed shape of the pipe at the last cycle of load application, with four-time magnification for (a) unreinforced chipped rubber-soil mixture, (b) unreinforced shredded rubber-soil mixture, (c) 5% rubber-soil mixture in reinforced installations

According to ASTM F949 (2006) [39] and ASTM D3034 (2008) [40] which focus on HDPE pipe and PVC sewer pipe respectively, the allowable deflection, as used in this study, is normally limited to 6-7.5% of the inside pipe diameter. The measured maximum vertical diameter changes of the S(5%)O mixture in the reinforced and unreinforced trenches are much smaller than the 6% deflection limit (about 1.84% and 3.68% of VDS for

S(5%)O-Re and S(5%)O-Ur respectively).

Thus, from the results described, using a mixture of 5% shredded rubber and soil in the "over" location of both unreinforced and unreinforced trenches, delivered the minimum soil surface settlement and pipe deflection among the other installations. So, from an engineering point of view, using the soil-rubber mixture with the specified rubber content can limit the pipe's accumulated

plastic deflections under repeated loading and also tends to decrease the soil surface settlement of the trench considerably. Taking this mixture as the preferred, composite, material, the effect of pipe stiffness is now studied.

#### 4.2. Pipe stiffness

In this section, the influence of pipe stiffness on the soil surface settlements, stress distribution with soil depth and stress distribution along the pipe's longitudinal axis are studied. In all cases, the backfill is assumed to be S(5%)O-Ur and the results are presented in the following sections.

In order to study the influence of pipe stiffness or of different kinds of pipe materials, tensile strengths of 1400, 560, 280, 140, 56, 1e-6 MPa were chosen for the buried pipe. The tensile 'strength' of 1e-6 is chosen as a device by which, in effect, a void is available instead of a pipe. Fig. 15a and 15b show the transferred vertical stresses and backfill settlements at the level of the pipe's crown (thus, on the pipe centerline the backfill settlement and pipe deformation are the same) respectively, with variation of

pipe stiffness. As can be seen, the stress on the pipe increases with increasing pipe stiffness. In fact, increasing the pipe stiffness make the stiffness of the middle part of the trench, where the pipe is, increased, i.e. more stress is carried by the pipe. The vertical stresses further increased away from the pipe's crown until it a point vertically above the pipe's side (80 mm from the pipe's centerline) and then decreased. The reason for this phenomenon is because of the increasing vertical stiffness of the pipe. On the other hand, if Fig. 15b is considered, the maximum settlements, for all stiffnesses, is found at the pipe's crown which, in effect, is acting something like a beam spanning, otherwise unsupported, between the pipe walls. Beyond the pipe's region, the stress decreased dramatically, and the settlements converged to a small value. The model also investigated the case which no pipe and with a pipe-sized void. In the absence of both pipe and void, the maximum stress was obtained on the centerline and then decreased gradually as the distance from the centerline increased. For the void condition the maximum stress was obtained above the soil alongside the void and, of course, was zero at the top of the void.

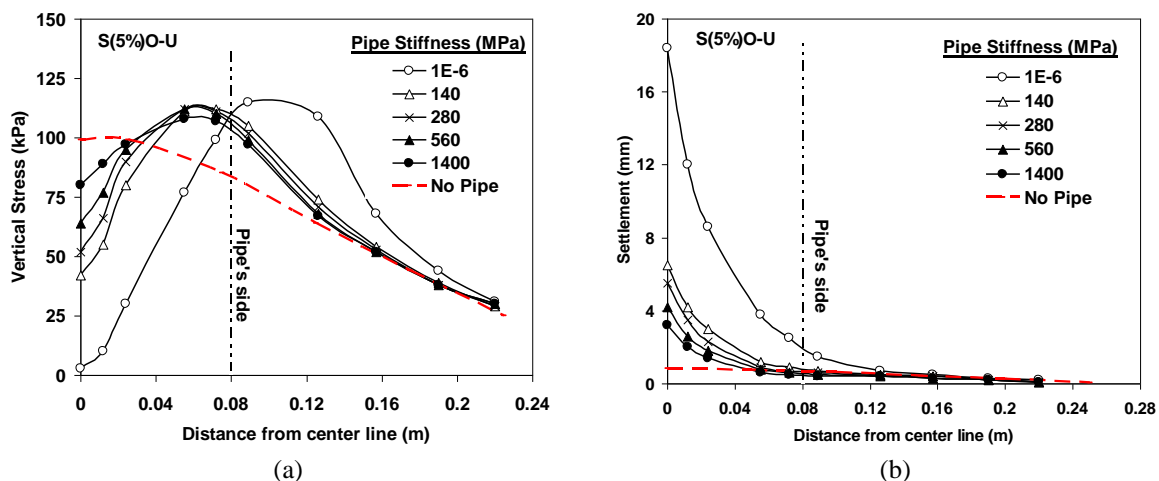


Fig. 15 Effect of pipe's stiffness on (a) transferred vertical stresses, (b) backfill settlement at the level of pipe's crown

Fig. 16 shows the stress distribution with trench depth for all pipes stiffnesses as well as for the no-pipe condition. The stress reduces in a very similar manner with depth for all installations until near the pipe's crown (about 8 cm above the crown), but the stress transferred to the crown reduces as the pipe's stiffness decreases inducing an arching effect in the trench backfill that takes results in a lower vertical stress immediately above the pipe. For example the stress on the pipe's crown for stiffnesses dropping from 1400 to 56 MPa reduced from 82 to 32 kPa (and to zero for the void case).

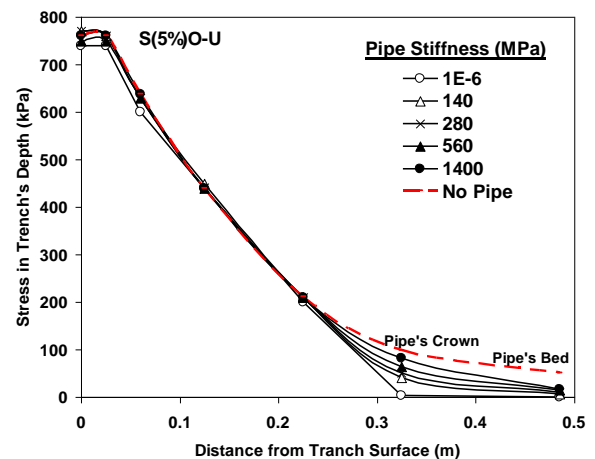
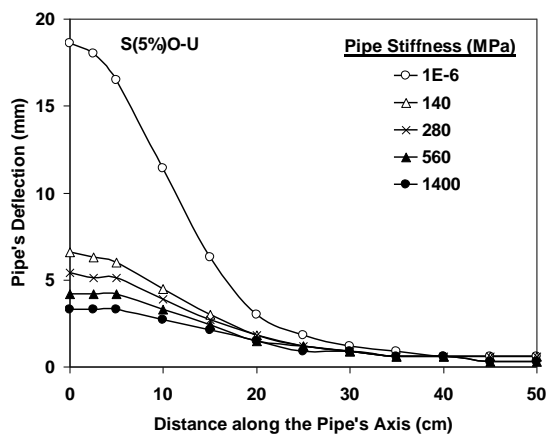


Fig. 16 Vertical stress distribution in trench depth from footing level to the trench bed

To gain a better assessment of the stress distribution area on the pipe, Fig. 17a was presented. This figure shows the variation of vertical pipe's deflection on its crown and along the pipe's longitudinal axis. The zero-value on the horizontal axis indicates the point on the crown immediately beneath the center of loading and the axis indicates the distance along the pipe's axis from that point. As expected, regardless of the pipe's stiffness, the deflection of the pipe's crown decreased away from the center of loading. Also, it is clear that the pipe's deflections for all pipe stiffnesses converge to the same minimum value over 30 cm distance from the centre of loaded area. Thus, as can be seen in Fig. 17b, the stress can be considered to be longitudinally distributed as per



Equation (1):

$$D = B + nH \quad (1)$$

Where,

$D$ : assumed equivalent diameter of stress distribution area based on the loaded length of the pipe's longitudinal axis

$B$ : Footing width or equivalent diameter of wheel print

$H$ : burial depth of the pipe

$n$ : load spreading factor which  $\approx 1.5$  for the depth of backfill,  $H=320\text{mm}$ , and wheel print diameter,  $B=150\text{mm}$ , used in the model cases tested here.

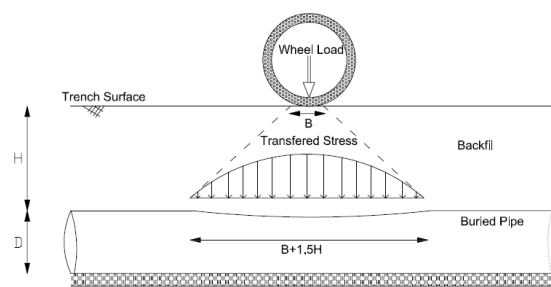


Fig. 17 Pipe deflection (a) for different pipes' stiffness, (b) along the pipe's longitudinal axis.

## 5. Summary and Conclusions

A series of numerical simulations was performed to simulate laboratory full-scale pipe-trench model tests by using a three-dimensional finite-difference program. The numerical model aimed to investigate the effects of installing geocell-reinforced layers over rubber-soil mixtures as an improved trench reinstatement technique and to assess the deformation characteristics of pipes with different stiffnesses. Rubber size/type, rubber content in the mixture, position of the mixture inside of the trench and level of repeated loading were varied as well as geocell reinforcement and unreinforced soil condition over the pipe to assess and evaluate the soil surface settlement and pipe deflection (especially at the pipe's crown). Fairly good agreement between the numerical and experimental results was observed. The findings derived from the modeling can be summarized as follows:

1) The geocell layer could reduce the spread and intensity of shear strain under the footing, tending to reduce both soil surface settlement and pipe deflection. With installation of a geocell-reinforced soil layer in the trench over the pipe, soil surface settlement and vertical diametral strain of pipe could be attenuated by 68% and 33% respectively in comparison with the value of the same parameters for an unreinforced trench.

2) The presence of the geocell layer beneath the loading surface changed the stress distribution in the

backfill, reducing its magnitude. So, by using a geocell just expanded over the trench width, not only is the buried pipe system considerably protected but, alternatively, pipes could be buried at a reduced depth, allowing installation costs to be substantially reduced.

3) Adding rubber particles, irrespective of size, with the exception of 5% shredded rubbers by weight, made the backfill more compressible than the soil alone and allowed greater deflection of the pipe and of the covering soil. However, the 5% shredded rubber mixed with the soil was found to act as a reinforcement material in the mixture so that the settlement of the backfill was reduced by 37% in comparison with the unreinforced and unmixed soil.

4) In general, the presence of a geocell reinforcement layer over the rubber-soil mixture, under repeated loading, tends to attenuate the pipe deflection both at crown and springline of the pipe and conceivably, may prevent the pipe from suffering a reversal of its curvature.

5) The influence of pipe stiffness on the soil surface settlements, stress distribution with soil depth and stress distribution along its longitudinal axis were studied. It was observed that the stress transferred onto the pipe's crown, reduces as the pipe's stiffness decreases due to the arching effect in the trench backfill. Also, an increase of the pipe wall's bending stiffness led to the vertical stresses increasing away from the pipe's crown until it reached a position above the pipe's side after which the vertical stresses decreased.

6) For the depth of burial investigated (320mm) the distribution of stress along the pipe's longitudinal axis, may be simulated by a circle area with a diameter equal to the load print diameter at the surface plus 1.5 times the burial depth of the pipe.

Further research is needed to validate the numerical model with the full-scale test data and field test data obtained from similar test conditions to adopt/extend this model for practical purposes and to real field scenarios. Also, to generalize the behavior of the pipe-trench system under the proposed improvement process, the effect of different sizes of pipe should be considered. In this study, repeated loadings were applied to simulate wheel loading of different vehicles. So, the authors recommend researchers to use high-frequency cyclic loading to achieve more realistic vehicle loadings. Also, using plasticity models with kinematic hardening rule is highly recommended to simulate the behavior of geocell-reinforced soil systems.

## References

- [1] Choo YW, Abdoun TH, O'Rourke MJ, Ha D. Remediation for buried pipeline systems under permanent ground deformation. *Soil Dynamics and Earthquake Engineering*, 2007, No. 12, Vol. 27, pp. 1043-1055.
- [2] Moghaddas Tafreshi SN, Tavakoli Mehrjardi Gh. Analysis of buried plastic pipes in reinforced sand under repeated-load using neural network and regression model, *International Journal of Civil Engineering, IJCE*, 2007, No. 2, Vol. 5, pp. 118-133.
- [3] Jafarzadeh F, Farahi Jahromi H, Abazari Torghabeh E. Investigating dynamic response of a buried pipeline in sandy soil layer by 1g shaking table test, *International Journal of Civil Engineering, IJCE*, 2010, No. 2, Vol. 8, pp. 107-124.
- [4] Collins KJ, Jensen AC, Mallinson JJ, Roenelle V, Smith IP. Environmental impact assessment of a scrap tyre artificial reef, *Journal of Marine Science and Engineering*, 2002, Vol. 59, pp. 243-249.
- [5] Humphrey DN, Katz LE. Five-year field study of the effect of tire shreds placed above the water table on groundwater quality, *J Transportation Research Record, Transportation Research Board*, 2000, Vol. 1714, pp. 18-24.
- [6] Feng ZY, Sutter KG. Dynamic properties of granulated rubber sand mixtures, *Geotechnical Testing Journal*, 2000, No. 3, Vol. 23, pp. 338-44.
- [7] Yoon S, Prezzi M, Siddiki NZ, Kim B. Construction of a test embankment using a sand-tire shred mixture as fill material, *Journal of Waste Management*, 2006, Vol. 26, pp. 1033-44.
- [8] Attom MF. The use of shredded waste tires to improve the geotechnical engineering properties of sands, *Environmental Geology*, 2006, Vol. 49, 497-503.
- [9] Edinçiler A, Avhan V. Influence of tire fiber inclusions on shear strength of sand, *J Geosynthetics International*, 2010, No. 4, Vol. 17, pp. 183-192.
- [10] Moghaddas Tafreshi SN, Tavakoli Mehrjardi Gh, Dawson AR. Buried pipes in rubber-soil backfilled trenches under cyclic loading, *Journal of Geotechnical and Geoenvironmental Engineering*, 2012, No. 11, Vol. 138, pp. 1346-56.
- [11] Thakur JK, Han J, Pokharel SK, Parsons RL. Performance of geocell-reinforced recycled asphalt pavement (RAP) bases over weak subgrade under cyclic plate loading, *J Geotextiles and Geomembranes*, 2012, Vol. 35, pp. 14-24.
- [12] Pokharel SK, Han J, Leshchinsky D, Parsons RL, Halahmi I. Investigation of factors influencing behavior of single geocell-reinforced bases under static loading, *J Geotextiles and Geomembranes*, 2010, No. 6, Vol. 28, pp. 570-578.
- [13] Sitharam TG, Sireesh S, Dash SK. Model studies of a circular footing supported on geocell-reinforced clay, *J Canadian Geotechnical Journal*, 2005, No. 2, Vol. 42, pp. 693-703.
- [14] Sitharam G, Sireesh ST, Dash SK. Performance of surface footing on geocell-reinforced soft clay beds, *Journal of Geotechnical and Geoenvironmental Engineering*, 2007, Vol. 25, pp. 509-524.
- [15] Moghaddas Tafreshi SN, Dawson AR. Comparison of bearing capacity of a strip footing on sand with geocell and with planar forms of geotextile reinforcement, *J Geotextiles and Geomembranes*, 2010a, Vol. 28, pp. 72-84.
- [16] Moghaddas Tafreshi SN, Dawson AR. Behaviour of footings on reinforced sand subjected to repeated loading - Comparing use of 3D and planar geotextile, *J Geotextiles and Geomembranes*, 2010b, Vol. 28, pp. 434-447.
- [17] Tavakoli Mehrjardi Gh, Moghaddas Tafreshi SN, Dawson AR. Combined use of geocell reinforcement and rubber-soil mixtures to improve performance of buried pipes, *J Geotextiles and Geomembranes*, 2012, No. 4, Vol. 34, pp. 116-130.
- [18] Tavakoli Mehrjardi Gh, Moghaddas Tafreshi SN, Dawson AR. Pipe response in a geocell reinforced trench and compaction considerations, *J Geosynthetics International*, 2013, No. 2, Vol. 20, pp. 105-18.
- [19] Babu GLS, Vasudevan AK, Haldar S. Numerical simulation of fiber-reinforced sand behaviour, *J Geotextiles and Geomembranes*, 2008, Vol. 26, pp. 181-88.
- [20] Saride S, Gowrisetti S, Sitharam TG, Puppala AJ. Numerical simulation of geocell-reinforced sand and clay, *J Ground Improvement*, 2008, No. G14, Vol. 162, pp. 185-98.
- [21] Leshchinsky B, Ling HI. Numerical modeling of behavior of railway ballasted structure with geocell confinement, *J Geotextiles and Geomembranes*, 2013, Vol. 36, pp. 33-43.
- [22] Brown SF, Brodrick BV. 25 years' experience with the pilot-scale nottingham pavement test facility, *International Conference on Accelerated Pavement Testing Reno, Nevada*, 1999, pp. 1-39.
- [23] American Society for Testing and Materials Standard practice for underground installation of thermoplastic pipe for sewers and other gravity-flow applications, *ASTM D 2321-08*, 2008.
- [24] British Standard Institute *Plastics pipework (thermoplastics materials): Code of practice for the installation of unplasticized PVC pipework for gravity drains and sewers*, BS 5955, 1980.
- [25] Moghaddas Tafreshi SN, Tavakoli Mehrjardi Gh. The use of neural network to predict the behaviour of small plastic pipes embedded in reinforced sand and surface settlement under repeated load, *Engineering Applications of Artificial Intelligence*, 2008, No. 6, Vol. 21, pp. 883-894.
- [26] *FLAC-3D Fast Lagrangian Analysis of Continua in Threedimensions*. ITASCA Consulting Group, Inc, Minneapolis, MN, 2002.
- [27] Rajagopal K, Krishanaswamy NR, Latha GM. Behaviour of sand confined with single and multiple geocells, *J Geotextiles and Geomembranes*, 1999, Vol. 17, pp. 171-84.

- [28] Zhang MX, Zhou H, Javadi AA, Wang ZW. Experimental and theoretical investigation of strength of soil reinforced with multi-layer horizontal-vertical orthogonal elements, *J Geotextiles and Geomembranes*, 2008, No. 1, Vol. 26, pp. 1-13.
- [29] Gotteland P, Lambert S, Balachowski L. Strength characteristics of tyre chips-sand mixtures, *J Studia Geotechnica et Mechanica*, 2005, Nos. 1-2, Vol. XXVII, pp. 55-66.
- [30] Erickson HL, Drescher A. Bearing capacity of circular footings, *J Geotechnical and Geoenvironmental Engineering*, 2002, No. 1, Vol. 128, pp. 38-43.
- [31] Moghaddas Tafreshi SN, Tavakoli Mehrjardi Gh, Ahmadi M. Experimental and numerical investigation on circular footing subjected to incremental cyclic loads, *International Journal of Civil Engineering, IJCE*, 2011, No. 4, Vol. 9, pp. 265-274.
- [32] Rogers CDF, Feleming PR, Loepky MWJ, Faragher E. The structural performance of profile-wall drainage pipe-stiffness requirements contrasted with the results of laboratory and field tests, *Journal of the Transportation Research Board*, 1995, Vol. 1514, pp. 83-92.
- [33] Werkmeister S, Dawson AR, Wellner F. Pavement design model for unbound granular materials, *Journal of Transportation Engineering*, 2004, No. 5, Vol. 13, pp. 665-674.
- [34] Arnold GK. Rutting of Granular Pavements, PhD Dissertation, University of Nottingham, 2004.
- [35] Rodriguez AR, Castillo HD, Sowers GF. *Soil Mechanics in Highway Engineering*, Trans Tech Publications Inc, 1988.
- [36] Garcya-Rojo R, Herrmann HJ. Shakedown of unbound granular material, *J Granular Matter*, 2005, No. 7, Vol. 7, pp. 109-111.
- [37] Werkmeister S, Dawson AR, Wellner F. Permanent deformation behavior of unbound granular materials and the shakedown theory, *Journal of the Transportation Research Board*, 2001, Vol. 1757, pp. 75-81.
- [38] Moser AP, Folkman S. *Buried Pipe Design*, McGraw-Hill Professional, 2008.
- [39] American Society for Testing and Materials. *Standard Specification for Poly (Vinyl Chloride) (PVC) Corrugated Sewer Pipe With a Smooth Interior and Fittings*, ASTM F 949-06, 2006.
- [40] American Society for Testing and Materials. *Standard Specification for Type PSM Poly(Vinyl Chloride) (PVC) Sewer Pipe and Fitting*, ASTM D 3034-08, 2008 s.